The Vibronic Structure of Electronic Absorption Spectra of Large Molecules: A Time-Dependent Density Functional Study on the Influence of "Exact" Hartree−Fock Exchange

Marc Dierksen and Stefan Grimme*

Theoretische Organische Chemie, Organisch-Chemisches Institut der Universität Münster, Corrensstrasse 40, D-48149 Münster, Germany

Received: June 22, 2004; In Final Form: August 24, 2004

The functional dependence of excited-state geometries and normal modes calculated with time-dependent density functional theory (TDDFT) is investigated on the basis of vibronic structure calculations of the absorption spectra of large molecules. For a set of molecules covering a wide range of different structures including organic dyes, biological chromophores, and molecules of importance in material science, quantum mechanical simulations of the vibronic structure are performed. In total over 40 singlet−singlet transitions of neutral closed-shell compounds and doublet−doublet transitions of neutral radicals, radical cations, and anions are considered. Calculations with different standard density functionals show that the predicted vibronic structure critically depends on the fraction of the "exact" Hartree−Fock exchange (EEX) included in hybrid functionals. The effect can been traced back to a large influence of EEX on the geometrical displacement upon excitation. On the contrary, the dependence of the results on the choice of the local exchange-correlation functional is found to be rather small. On the basis of detailed comparisons with experimental spectra conclusions are drawn concerning the optimum amount of EEX mixing for a proper description of the excited-state properties. The relationship of the quality of the simulated spectra with the errors for 0−0 transition energies is discussed. For the investigated singlet−singlet $\pi \rightarrow \pi^*$ transitions and the first strongly dipole-allowed transitions of PAH radical cations some rules of thumb concerning the optimum portion of EEX are derived. However, in general no universal amount of EEX seems to exist that gives a uniformly good description for all systems and states. Nevertheless an inclusion of about 30−40% of EEX in the functional is found empirically to yield in most cases simulated spectra that compare very well with those from experiment and thus seems to be necessary for an accurate description of the excited-state geometry. Pure density functionals that are computationally more efficient provide less accurate spectra in most cases and their application is recommended solely for comparison purposes to obtain estimates for the reliability of the theoretical predictions.

1. Introduction

In recent years time-dependent density functional theory (TDDFT)[1−3] has replaced the single excitation configuration interaction method (CIS) as the quantum chemical workhorse for calculating excitation energies and other excited-state properties of large molecules of up to 200 second-row atoms. For valence-excited states TDDFT reaches the accuracy of more sophisticated (and expensive) quantum chemical wave function methods. The problems inherent in the use of approximate ground-state exchange-correlation (xc) functionals for the calculation of Rydberg,[4,5] charge-transfer (CT)[6−9] and ionic valence-excited states[10−12] are well documented and are currently a very active field of research.

With the availability of analytical TDDFT gradients[13−15] a similar development is expected for the calculation of excited-state geometries and vibrational normal modes. Therefore an assessment of the quality of TDDFT calculations regarding these excited-state properties is of great interest. In contrast to the ground state, the excited-state geometries and normal modes are difficult to obtain experimentally in a direct way due to the short excited-state lifetimes. However, the vibronic structure of an electronic transition that can easily be measured contains information about the geometry and normal modes of the corresponding excited state. Vibronic structure calculations and comparisons with experimental data thus offer the possibility of an indirect assessment of the performance of the theoretical methods for the calculation of these excited-state properties.

Previous work[16] has shown for the first time that (TD)DFT calculations employing the popular B3-LYP functional yield a very good description of the vibronic structure of the absorption spectra for several larger organic π systems indicating the good quality of the excited-state geometries and normal modes. However, for the $1A_g \rightarrow 1B_u$ transition of octatetraene a rather strong dependence of the calculated vibronic structure on the density functional employed was observed.[17] Preliminary calculations on a few systems and employing several different functionals have shown that the displacement upon electronic excitation (the difference between the ground-state and the excited-state geometry), which is the central quantity for a simulation of the vibronic structure, strongly depends on the amount of "exact" Hartree−Fock exchange (EEX) included in the functional while the influence of the local part of the approximate xc functional used is rather small (see Section 3.2.3). A similar dependence has been observed earlier for the vertical excitation energies (ΔE^{vert})[3,18] indicating that there might

* Address correspondence to this author. Fax: (+49)251-83-36515. E-mail: grimmes@uni-muenster.de.

10.1021/jp047289h CCC: $27.50
Published on Web 10/14/2004

be a connection between these two phenomena. This raises the question whether the error for ΔE^{vert} obtained with different fractions of EEX can be used as an indicator for the amount of EEX that is necessary for a proper description of the excited-state geometry. However, since ΔE^{vert} does not correspond to any physical observable, i.e., cannot be extracted from an experimental spectrum, instead the errors for the 0−0 transition energies (ΔE^{0-0}) will be used here for this discussion.

In this work we present a detailed (TD)DFT study of the influence of EEX mixing on the quality of theoretical absorption spectra. A possible correlation of the quality of the simulated spectra with the errors for ΔE^{0-0} obtained with different amounts of EEX will be discussed. To be easily reproducible, the calculations have been performed with the standard functionals B-P86 (0% EEX), B3-LYP (20% EEX), and BH-LYP (50% EEX) which are implemented in most electronic structure program packages. A wide range of structurally different systems including organic dyes, biological chromophores, and molecules of importance in material science will be considered. This study should furthermore provide the reader with a comprehensive overview about the typical accuracy that can be obtained with TDDFT for electronic spectra simulations. Because over 40 different absorption spectra have been investigated in this study (which cannot all be shown), the results will be discussed by using some illustrative examples and the other spectra are included in the Supporting Information.

After a few words concerning the theory and technical details of the calculations in Section 2 an overview about the molecules and the corresponding electronic transitions considered will be given in Section 3.1. In Sections 3.2 and 3.3 the results for the investigated singlet−singlet and doublet−doublet transitions, respectively, will be presented.

2. Theory and Technical Details of the Calculations

Since the theory of vibronic transitions has been discussed earlier[16] only a few notes concerning the simulation of the vibronic spectra will be given here. All spectra shown in this study were calculated on the basis of the Franck−Condon (FC) approximation, i.e., vibronically induced transition dipole moments have been neglected. The error due to this treatment is expected to be small since nearly all transitions considered are strongly dipole allowed. For the weakly dipole-allowed transitions investigated the influence of vibronic coupling has been checked carefully and it was found to be negligible compared to the observed dependence on the different density functionals. In all vibronic structure calculations only the totally symmetric normal modes were considered. Test calculations have shown that nontotally symmetric modes can be discarded without introducing any significant error because the displacement upon excitation along these modes is zero and thus their contribution to the vibronic structure is small. Compared to an "exact" treatment the band structure is completely retained and the only effect observed is a small redistribution of spectral "underground" from higher energy regions to that near the 0−0 transition. Furthermore, it should be noted that the dependence of the calculated vibronic structure on the amount of EEX included in the functional will be exclusively discussed in terms of a dependence of the displacement upon excitation on EEX. The influence of EEX on the normal modes of the ground and excited state (more precisely, on the corresponding Duschinsky matrix) will not be discussed. This effect is expected to be small compared to the geometry dependence because the scaled vibrational frequencies and normal modes for the three functionals are very similar.

For all density functional calculations the TURBOMOLE 5.6[19] suite of programs was used. The functionals B-P86,[20,21] B3-LYP,[22,23] and BH-LYP[24] were applied in all calculations. Additionally, the functionals S-VWN,[25,26] B-LYP, PBE,[27,28] and PBE0[29] were tested. For the pure density functionals the RI approximation[30−32] was used. A Gaussian AO basis set of triple-ζ quality ([5s3p1d]/[3s1p], TZVP)[33] and a large grid for numerical quadrature ("grid 3" option) were employed and a tight SCF convergence criterium was chosen to avoid accumulation of numerical noise. The closed-shell systems were treated restricted while for the open-shell systems unrestricted (TD)-DFT calculations were performed. For the open-shell compounds the $\langle S^2 \rangle$ values of the ground-state Kohn−Sham determinant obtained with the B−P86 functional lie in the range of 0.75−0.77 indicating that the spin-contamination is only small, which is in line with previous findings for pure DFT functionals. As expected, for the hybrid functionals with increasing admixture of EEX larger $\langle S^2 \rangle$ values of 0.76−0.79 (B3-LYP) and 0.78−0.87 (BH-LYP) are found. With all three functionals applied the neutral radicals showed the largest $\langle S^2 \rangle$ values. The geometries of the ground and excited states were optimized by using analytical DFT and TDDFT[15,34] gradients, respectively. The normal coordinates and frequencies of both states were obtained numerically by (two-side) finite difference of the analytical gradients using an extended version of the program SNF 2.2.1[35,36] running in parallel on a LINUX PC-cluster. The frequencies of both the ground- and excited-state normal modes were scaled with the same factor of 0.9614 (B3-LYP and BH-LYP) and 0.9914 (B-P86), respectively.[37] All combinations of vibrational quanta in the energy range of interest were generated and the intensities of the corresponding vibronic transitions were calculated with the program FCfast 0.9.[38] For comparison with the experimental spectra the obtained intensities were broadened by using Gaussian or Lorentzian shape functions with a constant half-width that was adjusted manually to match the corresponding experimental spectrum. The experimental and calculated spectra were normalized to the signal of highest intensity and ΔE^{0-0} was set to zero.

Finally, we want to give some brief notes on the computational cost of our approach. The excited-state optimization is about 1−2 times as costly as the corresponding ground-state calculation and the scaling with the system size is the same. The rate determining step of the entire simulation procedure is the numerical calculation of the vibrational modes for both states, which for the larger systems studied took a few days in parallel on 8 Pentium IV 2.4 GHz nodes.

3. Results and Discussion

3.1. Overview. An overview about the closed- and open-shell molecules considered in this study with the numbering that will be used as reference in the following discussion is shown in Figures 1 and 2, respectively. For all electronic transitions the symmetry of the ground and excited state, the calculated vertical excitation energy ΔE^{vert}, the experimental ΔE^{0-0} values, and the errors for ΔE^{0-0} obtained with the different functionals are given in Table 1. Note that the experimental ΔE^{0-0} values for those transitions which have been measured in solution or matrix have been increased by 0.15 eV to account for a solvent-induced red shift of ΔE^{0-0}. For the systems with D_{2h} symmetry a molecular orientation in the *xy*-plane with the long axis along the *x*-direction is taken; molecules with C_{2v} symmetry are aligned with the long axis along the *x*-direction. The errors for ΔE^{0-0} are also presented graphically in Figure 3, which will be used in the following to discuss a

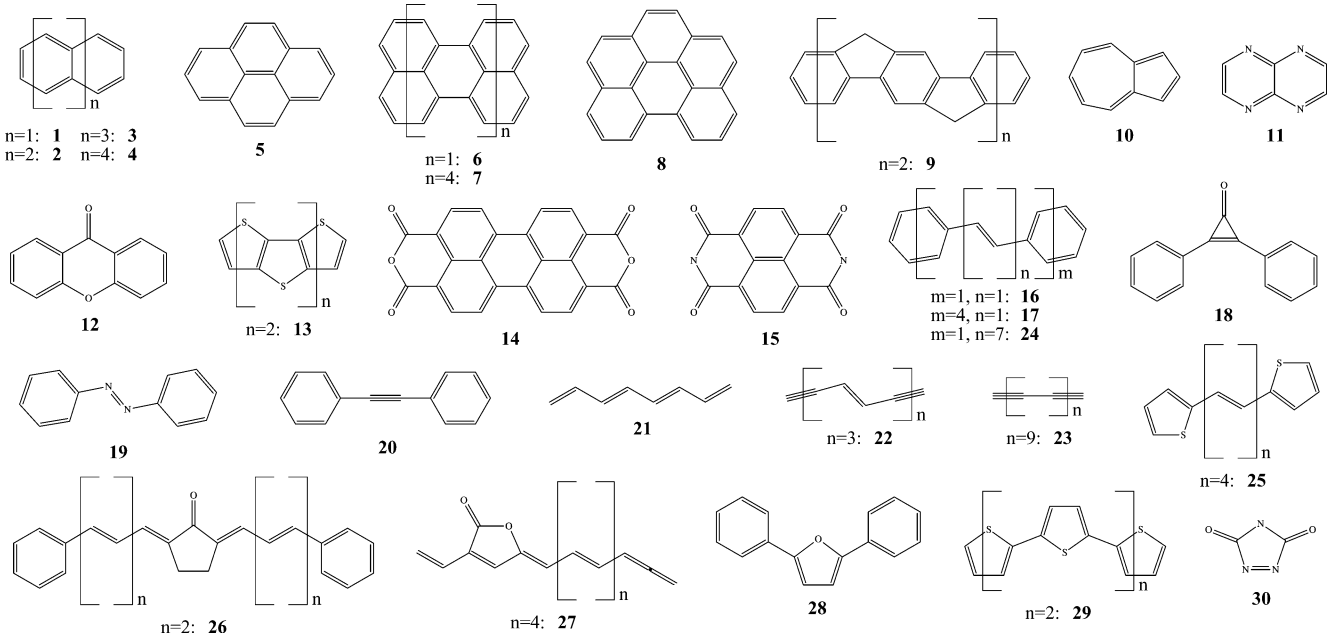

Figure 1. Overview of the closed-shell molecules considered in this study with the numbering that will be used as reference in the text.

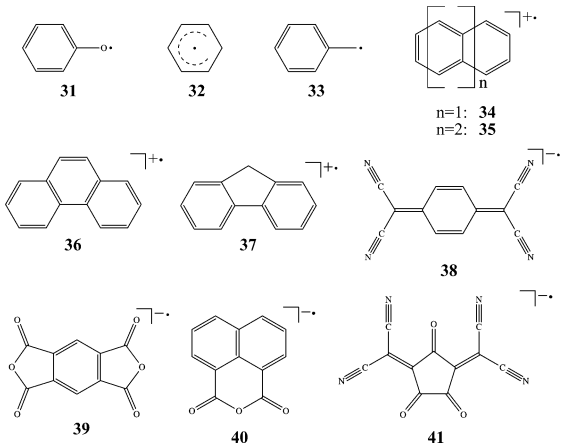

Figure 2. Overview of the open-shell molecules considered in this study with the numbering that will be used as reference in the text.

possible relationship of the quality of the spectrum on one hand and the errors for ΔE^{0-0} with different amounts of EEX on the other. It should be mentioned that for some of the systems studied here one or more imaginary frequencies were obtained for nontotally symmetric normal modes. Test calculations show that in some cases the barrier of the corresponding double-minimum potentials cannot be regarded as negligible compared to the vibrational energy, which should have an effect on the vibronic structure. However, simulations for these systems with the symmetry-broken geometries corresponding to the real (TD)-DFT minima clearly show significant deviations from experiment indicating that the imaginary frequencies are very likely artifacts of the (TD)DFT treatments. Therefore in the following the geometries in the higher symmetry as denoted in Table 1 were used for the simulation of the vibronic spectra.[39]

3.2. Singlet−Singlet Transitions. *3.2.1. Polycyclic Aromatic Hydrocarbons (PAH) and Rigid Homoaromatic Systems.* The first strongly dipole allowed singlet−singlet transition of the linear-condensed acenes ($S_0 \rightarrow S_2$ for naphthalene, $S_0 \rightarrow S_1$ for the other acenes) has been studied extensively both with experimental and theoretical methods and can be regarded as a prototype for $\pi \rightarrow \pi^*$ transitions of aromatic compounds. As first examples we thus want to discuss the results for the homologous acenes naphthalene (**1**), anthracene (**2**), tetracene (**3**), and pentacene (**4**). The excited states can (in an orbital picture) be described as a promotion of one electron from the highest occupied molecular orbital to the lowest unoccupied molecular orbital (HOMO → LUMO transition) and in the Platt nomenclature (perimeter model)[42] is denoted as the L_a state. Figure 4 shows a comparison of the calculated and experimental spectra for **1** and **3**. With increasing amount of EEX included in the functional a shift of intensity from the 0−0 transition to higher energy regions can be observed indicating an increase of the geometric displacement upon excitation. Compared to experiment, both B-P86 and B3-LYP seem to underestimate the displacement upon excitation while it is overestimated with the BH-LYP functional. This suggests that about 30% EEX would be optimum for the acenes, which is supported by the results obtained for **2** and **4** (see Supporting Information). For an assessment of the basis set dependence additional calculations have been performed for **3** with the B3-LYP functional applying basis sets of double-ζ quality ([3s2p1d]/[2s1p], SVP),[43] triple-ζ quality with two ([5s3p2d1f]/[3s2p1d], TZVPP) and three sets ([5s3p3d2f1g]/[3s3p2d1f], TZVPPP) of polarization functions, and also quadruple-ζ quality ([7s4p3d2f1g]/[4s3p2d1f], QZ-VP).[44] Compared to the spectrum obtained with our standard triple-ζ basis set, the simulation with the double-ζ basis set shows a small decrease of the displacement (see Figure 4) while the larger basis sets yield almost identical results (example of QZVP given in Figure 4). This suggests that the basis set of triple-ζ quality used is close the basis set limit (for this type of application). The absolute (signed) errors for ΔE^{0-0} with the different functionals decrease (increase) monotonically with increasing amount of EEX and the BH-LYP functional yields the best agreement with the experimental values (see Figure 3 and Table 1) in contrast to the results for the simulated spectra. Therefore, no correlation of the quality of the calculated spectrum and the error for ΔE^{0-0} is found for the acenes. Similar observations for the L_a ($S_0 \rightarrow S_2$) transition of pyrene (**5**) (see the Supporting Information) indicate that these conclusions can also be transferred to L_a states of other PAH.

To put this conclusion on a more solid basis, the L_a ($S_0 \rightarrow S_1$) transitions of the larger PAH perylene (**6**), pentarylene (**7**), and benzoperylene (**8**) have been investigated. A comparison

TABLE 1: Comparison of ΔE^{vert}, the Experimental ΔE^{0-0}, and the Errors for ΔE^{0-0} (ΔE^{0-0}(calcd) − ΔE^{0-0}(exptl)) Obtained with the Functionals B-P86, B3-LYP, and BH-LYP for the Investigated Electronic Transitions (in eV)[a]

		ΔE^{vert}			ΔE^{0-0}	ΔE^{0-0}(calcd) − ΔE^{0-0}(exptl)		
molecule	transition	B-P86	B3-LYP	BH-LYP	exptl	B-P86	B3-LYP	BH-LYP
1	$1^1A_g \rightarrow 1^1B_{2u}$	4.07	4.40	4.82	4.44[40]	−0.72	−0.46	−0.07
2	$1^1A_g \rightarrow 1^1B_{2u}$	2.90	3.25	3.69	3.41[40]	−0.77	−0.51	−0.12
3	$1^1A_g \rightarrow 1^1B_{2u}$	2.14	2.47	2.91	2.76[b,41]	−0.83	−0.58	−0.20
4	$1^1A_g \rightarrow 1^1B_{2u}$	1.61	1.93	2.35	2.28[b,71]	−0.84	−0.61	−0.24
5	$1^1A_g \rightarrow 1^1B_{3u}$	3.37	3.69	4.10	3.84[40]	−0.68	−0.42	−0.11
6	$1^1A_g \rightarrow 1^1B_{3u}$	2.53	2.82	3.22	3.11[b,45]	−0.83	−0.62	−0.30
7	$1^1A_g \rightarrow 1^1B_{3u}$	1.37	1.56	1.89	1.81[b,46]	−0.56	−0.37	−0.20
8	$1^1A_1 \rightarrow 1^1B_1$	2.88	3.22	3.67	3.37[b,72]	−0.69	−0.39	−0.06
9	$1^1A_g \rightarrow 1^1B_u$	2.50	3.00	3.52	3.11[b,73]	−0.80	−0.41	0.10
10	$1^1A_1 \rightarrow 1^1B_1$	2.30	2.40	2.54	1.93[b,74]	−0.07	0.06	0.24
11	$1^1A_g \rightarrow 1^1B_{3u}$	4.27	4.52	4.86	4.02[b,75]	0.05	0.31	0.62
12	$1^1A_1 \rightarrow 2^1A_1$	3.43	3.93	4.61	3.81[76]	−0.52	−0.14	0.56
13	$1^1A_1 \rightarrow 1^1B_1$	3.23	3.52	3.93	3.62[b,77]	−0.63	−0.42	−0.13
14	$1^1A_g \rightarrow 1^1B_{3u}$	2.14	2.43	2.84	2.52[b,48]	−0.56	−0.29	0.01
15	$1^1A_g \rightarrow 1^1B_{3u}$	3.00	3.38	3.88	3.40[b,78]	−0.61	−0.27	0.12
16	$1^1A_g \rightarrow 1^1B_u$	3.60	3.90	4.29	3.92[b,54]	−0.63	−0.40	−0.13
17	$1^1A_g \rightarrow 1^1B_u$	2.03	2.55	3.14	2.95[b,55]	−1.06	−0.63	−0.16
18	$1^1A_1 \rightarrow 1^1B_1$	3.59	4.00	4.53	4.05[b,79]	−0.86	−0.45	0.12
19	$1^1A_g \rightarrow 1^1B_u$	3.38	3.75	4.26	3.64[b,80]	−0.62	−0.33	0.01
20	$1^1A_g \rightarrow 1^1B_{3u}$	3.79	4.13	4.57	4.31[b,79]	−0.77	−0.55	−0.20
21	$1^1A_g \rightarrow 1^1B_u$	3.77	4.05	4.47	4.41[81]	−0.86	−0.70	−0.39
22	$1^1A_g \rightarrow 1^1B_u$	2.68	3.03	3.56	3.37[b,50]	−0.83	−0.55	−0.18
23	$1^1\Sigma_g^+ \rightarrow 1^1\Sigma_u^+$	2.83	3.28	4.14	3.69[b,c,51]	−0.95	−0.58	0.21
24	$1^1A_g \rightarrow 1^1B_u$	2.05	2.38	2.96	2.71[b,82]	−0.80	−0.53	−0.12
25	$1^1A_g \rightarrow 1^1B_u$	2.44	2.75	3.26	3.10[b,83]	−0.82	−0.59	−0.22
26	$1^1A_1 \rightarrow 1^1B_1$	2.02	2.52	3.18	3.14[b,84]	−1.16	−0.76	−0.28
27	$1^1A' \rightarrow 2^1A'$	2.17	2.47	3.01	2.71[b,53]	−0.69	−0.43	−0.06
28	$1^1A_1 \rightarrow 1^1B_1$	3.36	3.68	4.10	3.75[b,41]	−0.64	−0.38	−0.10
29	$1^1A_1 \rightarrow 1^1B_1$	2.17	2.52	3.02	2.77[b,55]	−0.76	−0.50	−0.14
30	$1^1A_1 \rightarrow 1^1B_2$	1.67	2.03	2.45	2.32[b,56]	−0.90	−0.51	−0.07
31	$1^2B_2 \rightarrow 1^2A_2$	2.07	2.38	2.97	2.12[b,57]	−0.37	0.02	0.59
32	$1^2B_2 \rightarrow 2^2A_2$	3.80	3.98	4.39	4.05[b,58]	−0.48	−0.20	0.17
33	$1^2B_2 \rightarrow 2^2A_2$	3.50	3.88	4.53	4.04[b,64]	−0.70	−0.34	0.35
34	$1^2A_u \rightarrow 1^2B_{3g}$	2.11	2.15	2.16	1.97[b,59]	−0.06	0.01	−0.02
35	$1^2B_{3g} \rightarrow 1^2A_u$	1.86	1.94	2.09	1.87[b,85]	−0.11	−0.06	0.07
36	$1^2B_2 \rightarrow 1^2A_2$	1.60	1.66	1.75	1.53[b,60]	−0.09	−0.07	−0.02
37	$1^2A_2 \rightarrow 1^2B_2$	2.15	2.23	2.37	2.11[b,62]	−0.12	−0.07	0.05
38	$1^2B_{2g} \rightarrow 1^2B_{1u}$	1.73	1.78	1.75	1.62[b,63]	−0.01	0.00	−0.18
39	$1^2A_u \rightarrow 1^2B_{3g}$	1.94	2.06	2.29	2.01[b,64]	−0.16	−0.04	0.19
	$1^2A_u \rightarrow 1^2B_{2g}$	3.30	3.45	3.38	3.34[b,64]	−0.36	−0.20	−0.32
40	$1^2A_2 \rightarrow 1^2B_2$	1.62	1.58	1.78	1.46[b,86]	−0.03	0.01	0.09
	$1^2A_2 \rightarrow 3^2A_2$	3.10	3.33	3.52	3.16[b,64]	−0.23	−0.04	0.07
41	$1^2B_2 \rightarrow 1^2A_2$	2.44	1.83	1.94	1.72[b,87]	−0.13	−0.01	0.14

[a] The conventions concerning the orientation of the molecules with D_{2h} and C_{2v} symmetry are given in the text. [b] The excitation energy has been increased by 0.15 eV to account for a solvent-induced red shift. [c] Additionally, the value has been increased by 0.18 eV to account for the red shift due to the TIPS end caps (see Section 3.2.3).

of the simulated spectra of **6** and **7** with experiment is shown in Figure 5. As for the acenes, the displacement upon excitation increases with the amount of EEX included in the functional. For **6** the spectrum obtained with B3-LYP shows an almost perfect agreement with that from experiment. The B-P86 functional slightly underestimates the displacement while it is clearly too large with BH-LYP.

Since **7** is a higher homologue of **6** similar results are expected for this compound. However, as can be seen from Figure 5, the spectrum obtained with BH-LYP clearly shows the best agreement with experiment and both B3-LYP and B-P86 provide not enough intensity in the high-energy regions. These results indicate that for the rylenes the optimum amount of EEX increases with the number of naphthalene units in the molecule. Unfortunately, it seems thus not possible to extrapolate the results for small systems to larger compounds even when they seem structurally similar.

For **8** B3-LYP shows an underestimation and BH-LYP on the other hand an overestimation of the displacement (see the Supporting Information) and thus about 30% of EEX is expected

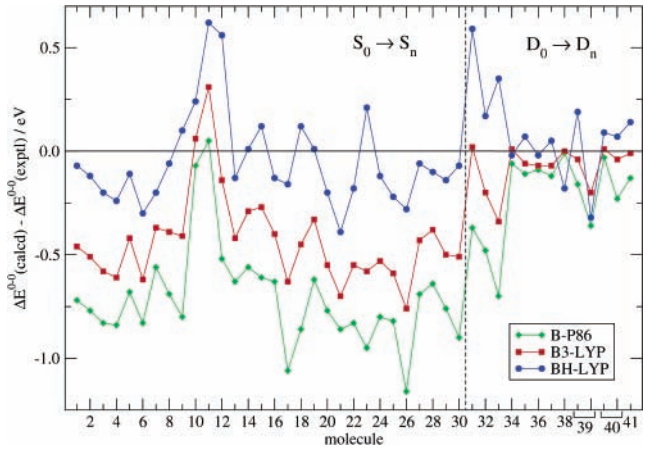

Figure 3. Errors for ΔE^{0-0} (ΔE^{0-0}(calcd) − ΔE^{0-0}(exptl)), in eV, obtained with the functionals B-P86, B3-LYP, and BH-LYP. The results for the singlet−singlet and doublet−doublet transitions are shown on the left and right sides of the plot, respectively.

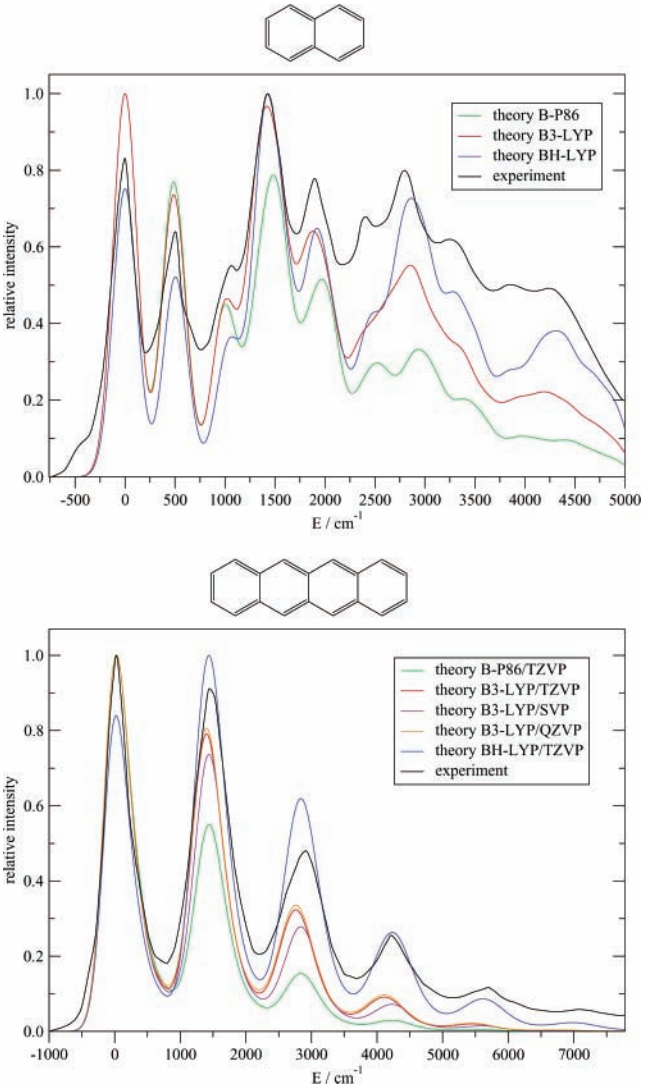

Figure 4. Top panel: Comparison of the calculated and experimental[40] absorption spectra for the $1^1A_g \rightarrow 1^1B_{2u}$ (L_a) transition of naphthalene (**1**). Bottom panel: Comparison of the calculated and experimental[41] absorption spectra for the $1^1A_g \rightarrow 1^1B_{2u}$ (L_a) transition of tetracene (**3**).

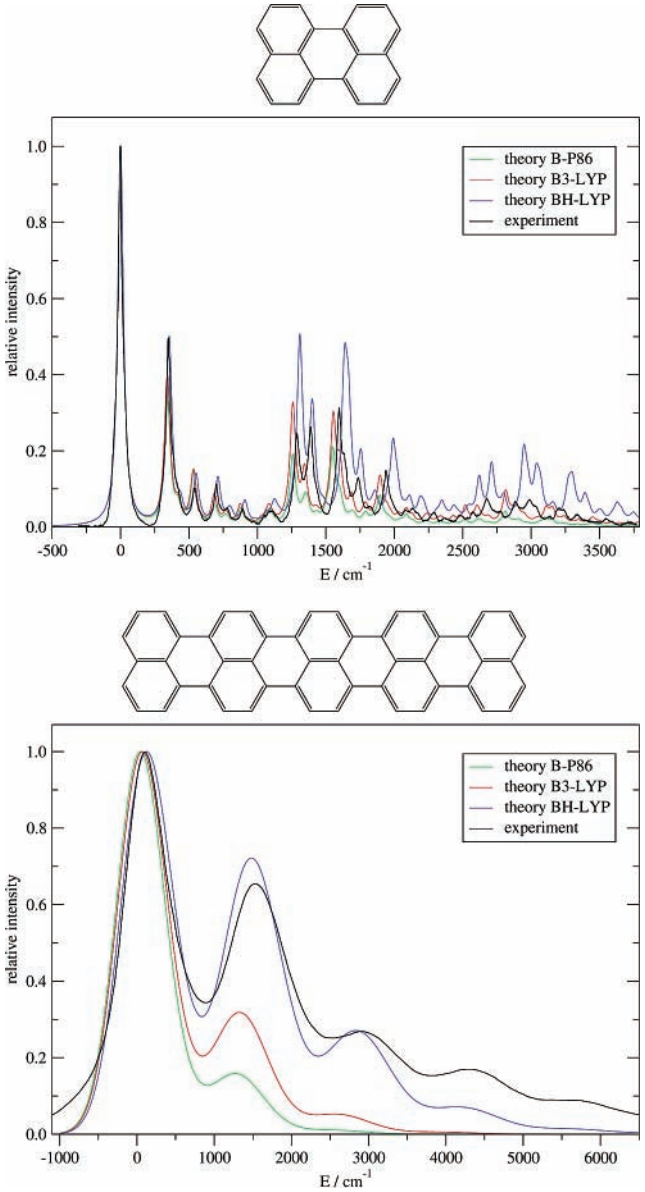

Figure 5. Top panel: Comparison of the calculated and experimental[45] absorption spectra for the $1^1A_g \rightarrow 1^1B_{3u}$ (L_a) transition of perylene (**6**). Bottom panel: Comparison of the calculated and experimental[46] absorption spectra for the $1^1A_g \rightarrow 1^1B_{3u}$ (L_a) transition of pentarylene (**7**).

to be optimum as for the acenes. As seen in Figure 3 and Table 1 no connection between the quality of the simulated spectrum and the error for ΔE^{0-0} is found for **6** and **8** and thus the correlation observed for **7** has to be regarded as more or less incidental since it is known[10,11] that the absolute error for ΔE^{0-0} of ionic states (in a valence-bond picture) generally decreases with the amount of EEX included in the functional.

The results obtained for the L_a ($S_0 \rightarrow S_1$) transition of **9** that contains repeating biphenyl units show a slight overestimation of the displacement with BH-LYP (see the Supporting Information) indicating that about 40% of EEX would probably yield the best agreement with experiment. As seen from Figure 3 and Table 1 a similar fraction of EEX is expected to give an accurate estimation for ΔE^{0-0}. Thus, for this system the quality of the simulated spectrum and the errors for ΔE^{0-0} with different amounts of EEX seem to correlate.

All the systems presented so far show a systematic increase of the displacement upon excitation with the amount of EEX included in the functional. For the L_a ($S_0 \rightarrow S_1$) transition of azulene (**10**), however, the B-P86 and B3-LYP functionals give almost identical results that are both in excellent agreement with experiment (see Supporting Information) while the displacement is clearly *underestimated* with BH-LYP. This indicates that the pronounced differences observed for the ground-state properties of **10** compared to its alternating isomer **1** (e.g., symmetry breaking to a C_s structure with HF, see ref 47) also transfer to the electronic structure of the excited state. Furthermore, concerning the errors of ΔE^{0-0}, for all alternating PAH presented so far the BH-LYP functional yields the best results (as expected for ionic L_a states) while for the L_a state of **10**, BH-LYP shows the largest error of 0.24 eV (Figure 3 and Table 1). For **10** a portion of about 10% EEX would yield the best agreement with experiment and thus there seems to be a correlation of the quality of the simulated spectrum with the error for ΔE.$^{0-0}$

3.2.2. Rigid Heteroaromatic Systems. All compounds considered so far are plain hydrocarbons and therefore little charge transfer between the atoms in one state as well as no change of charge-transfer character between the ground and the excited state is involved. Since almost all "real-life" systems include one or more heteroatoms which can have a strong effect on the

photophysical properties, in the following the results obtained for a number of heteroaromatic systems will be discussed.

For the L_a state of tetraazanaphthalene (**11**) B-P86 clearly underestimates the geometric displacement upon excitation. With the B3-LYP and BH-LYP functionals similar results are obtained for the displacement but only the B3-LYP calculation yields an accurate description of the relative intensities of the peaks at 700 and 1400 cm^{-1}, respectively (see the Supporting Information). In this case the functional dependence can partially also be attributed to differences of the excited-state normal modes. The BH-LYP and B3-LYP functionals both overestimate ΔE^{0-0} (errors of 0.62 and 0.31 eV, respectively) while the B-P86 functional yields the best agreement with the experimental value (error of 0.05 eV). Thus for **11** clearly no correlation of the results for the simulated spectrum with the errors for ΔE^{0-0} is found.

The results obtained for the L_a ($S_0 \rightarrow S_2$) transition of xanthone (**12**) are similar for the three functionals used except for a systematic frequency shift observed for BH-LYP (see the Supporting Information). Since the experimental phosphorescence excitation spectrum seems to exhibit significant background noise, no conclusions regarding an optimum amount of EEX for the simulation of the spectrum can be drawn. The B-P86 functional underestimates ΔE^{0-0} by more than 0.5 eV, BH-LYP yields an overestimation by about the same amount, while the B3-LYP functional shows the best agreement with the experimental value (error of -0.14 eV). This, however, is in clear contrast to the rather small differences found for the calculated vibronic structure.

For the L_a transition of **13** an underestimation of the displacement is observed with B-P86 and B3-LYP while BH-LYP slightly overestimates the displacement upon excitation (see the Supporting Information). Out of the three functionals BH-LYP yields the best agreement with the experimental ΔE^{0-0} value (error of -0.13 eV).

The simulations for the L_a state of **14** lead to similar conclusions as for **13** (see the Supporting Information). Compared to **6** a larger amount of EEX seems to be necessary. It should be noted that calculations for this system employing a tight-binding version of DFT with the PBE functional[48] yield a significant *overestimation* of the displacement. Since our calculations show that PBE performs similar to B-P86 this can probably be traced back to the tight-binding approximation used. The ΔE^{0-0} value is predicted very accurately with the BH-LYP functional (error of 0.01 eV, see Figure 3 and Table 1) in contrast to the observation for the calculated spectra.

The simulations performed for the L_a state of **15** again yield an underestimation of the displacement with B-P86 and B3-LYP while the BH-LYP functional shows an overestimation as in the previous examples (see the Supporting Information). It should be noted here that the absorption spectrum has been simulated exclusively on the basis of the vibronic structure obtained for the L_a state. Contributions from the weakly dipole-allowed L_b transition, which lies about 1200 cm^{-1} higher in energy,[49] are swamped by the vibronic structure of the more intense L_a transition and are expected to have only a small effect on the observed band shape. The errors for ΔE^{0-0} indicate that about 40% of EEX would be optimum in agreement with the results for the simulated spectra.

3.2.3. Flexible Hydrocarbons Consisting of Alternating Double and Triple Bonds. All the examples discussed so far are built from condensed aromatic units and can thus be regarded as structurally rather rigid. Chromophores of biological and technical interest on the other hand often include a number of conjugated double or triple bonds. Besides an increased flexibility these molecules are also expected to show a different behavior upon excitation due to the lack of aromaticity. After a discussion of the systems built exclusively from double or triple bonds, several mixed compounds containing both nonaromatic and aromatic parts will be presented in the next section.

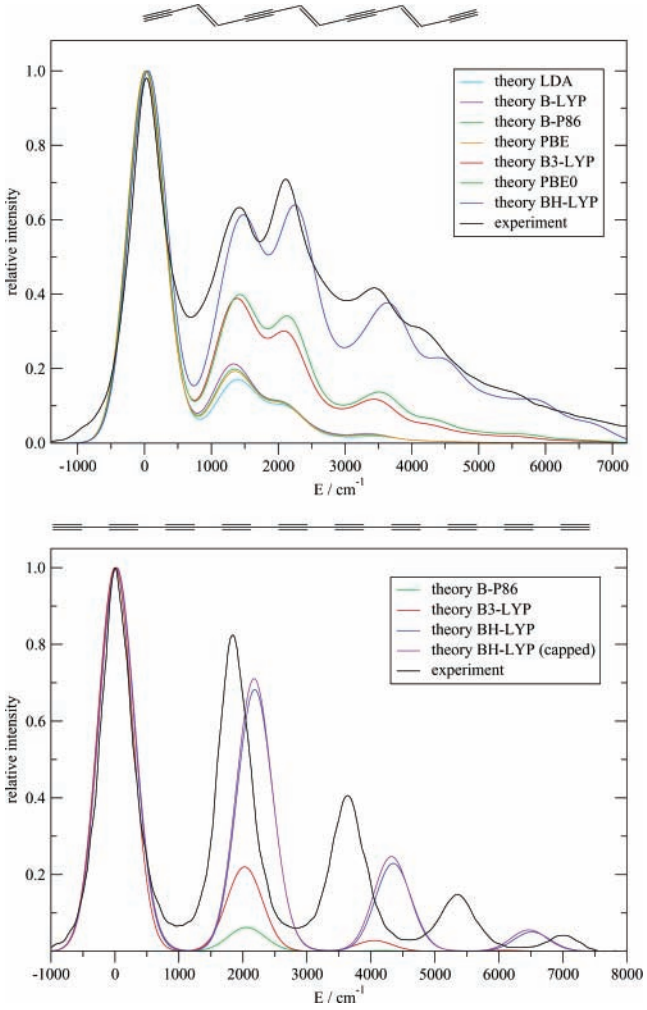

Figure 6. Top panel: Comparison of the calculated and experimental[50] absorption spectra for the $1^1A_g \rightarrow 1^1B_u$ transition of **22**. The simulated spectrum obtained with the S-VWN functional is shown as an example for the calculations performed with different LDA functionals. Bottom panel: Comparison of the calculated spectra for the $1^1\Sigma_g^+ \rightarrow 1^1\Sigma_u^+$ transition of decayne (**23**) with the experimental absorption spectrum of the TIPS end-capped derivative.[51] Additionally the calculated spectrum for the $1^1A_1' \rightarrow 1^1A_2''$ excitation of the TMS end-capped derivative employing the BH-LYP functional is included.

The simulations for the $1A_g \rightarrow 1B_u$ state of octatetraene (**21**) show a clear underestimation of the displacement with B-P86. The B3-LYP functional also seems to underestimate this effect while BH-LYP yields a slight overestimation[52] (see the Supporting Information). For the ΔE^{0-0} values the BH-LYP functional yields the best agreement with experiment. Nevertheless, the error is still about 0.4 eV indicating that an even larger portion of EEX would be optimum.

For the strongly dipole-allowed $1A_g \rightarrow 1B_u$ transition of the oligomer **22** that corresponds to the well-studied $1A_g \rightarrow 1B_u$ transition of polyenes simulations have been performed with several different functionals. The comparison of the calculated and experimental spectra presented in Figure 6 clearly shows a large influence of EEX while for the pure DFT functionals almost identical results are obtained indicating that the depen-

dence on the local part of the approximate xc-functional used is rather small. As for most of the aromatic examples discussed above an increase of the displacement upon excitation with the fraction of EEX in the functional can be observed although the dependence seems to be even larger. Both B-P86 and B3-LYP yield a clear underestimation of the displacement while the spectrum calculated with BH-LYP shows an excellent agreement with experiment. The same holds for the calculated ΔE^{0-0} values (see Figure 3 and Table 1).

Figure 6 shows a comparison of the simulated spectra for the strongly dipole-allowed $1\Sigma_g^+ \rightarrow 1\Sigma_u^+$ transition of decayne (**23**) with the experimental absorption spectrum of the triisopropylsilyl (TIPS) end-capped derivative. Obviously the frequency of the C−C stretch vibration is systematically overestimated with all three functionals. As in the example before, the B-P86 and B3-LYP functionals yield a too small displacement. Although the BH-LYP functional shows the best agreement with experiment we note that an even larger amount of EEX seems to be necessary for a quantitative description of the experimental spectrum. For an assessment of the effects of the TIPS group on the photophysical properties additional calculations have been performed for the trimethylsilyl (TMS) end-capped derivative of **23**. The TDDFT calculations with the three functionals yield a small decrease for ΔE^{vert} compared to the uncapped system of 0.21 (B-P86), 0.19 (B3-LYP), and 0.15 eV (BH-LYP), respectively. Furthermore, for the simulated spectrum only a slight increase of the displacement can be observed (see Figure 6). Therefore the influence of the TIPS groups seems to be rather small and **23** is expected to be a good model system. In contrast to the results obtained for the simulated spectra, the errors for ΔE^{0-0} indicate that about 40−50% EEX would give the best agreement with experiment. It should be noted that the experimental ΔE^{0-0} given in Table 1 has been increased by 0.18 eV (in addition to the solvent correction) to account for the effect of the TIPS substituents.

Comparing the results for **21**, **22**, and **23**, the dependence of the displacement on the amount of EEX seems to be larger for systems with triple than for those with double bonds and it seems that triply bonded systems require a larger fraction of EEX. Furthermore, regarding the results for ΔE^{0-0} the influence of EEX seems to be larger for compounds with triple bonds (Figure 3 and Table 1) as seen for the displacement. The optimum portion of EEX, however, seems to be smaller for triply bonded systems in contradiction to the results obtained for the displacement.

3.2.4. "Real-Life" Systems. For the aromatic systems discussed so far we have seen that an amount of 30−40% EEX yields overall the best agreement between theoretical and experimental spectra while for compounds consisting of conjugated double or triple bonds a larger portion of about 50−60% EEX should be included in the functional. For "real-life" systems which generally contain both aromatic moieties and conjugated double or triple bonds the optimum fraction of EEX is expected to depend on the ratio of the two different subunits. In the following the results obtained for several of such mixed systems are presented.

For the strongly dipole-allowed $1A_g \rightarrow 1B_u$ transition of **24** the spectrum calculated with the BH-LYP functional shows the best agreement with experiment (see the Supporting Information). However, comparison with the B3-LYP data indicates that about 40% EEX would yield even better results. On the contrary, the errors for ΔE^{0-0} (Figure 3 and Table 1) show that EEX should be larger than 50%. Similar results are obtained for the strongly dipole-allowed $1A_g \rightarrow 1B_u$ transition of **25** (see the Supporting Information). The calculations for the $1A_1 \rightarrow 1B_1$ transition of **26** again show a significant underestimation of the displacement both with B-P86 and B3-LYP while the BH-LYP functional yields an excellent agreement with experiment (see the Supporting Information). Again, the ΔE^{0-0} value with BH-LYP is still too low by about 0.3 eV and a larger amount of EEX seems necessary.

The polyene derivative **27** represents a model system for the biological chromophore peridinine found in an antenna pigment−protein complex used by dinoflagellates species for harvesting light energy.[53] The simulated spectra for the strongly dipole-allowed $1A' \rightarrow 2A'$ transition of **27** show a significant underestimation of the displacement with B-P86 and B3-LYP (see the Supporting Information) as expected for a compound with a large number of conjugated double bonds. The calculation with the BH-LYP functional is in good agreement with experiment and furthermore BH-LYP also gives the best result for ΔE^{0-0} (error of −0.06 eV). From the last four examples one can conclude that for the simulation of the spectrum the optimum fraction of EEX in the functional can indeed be estimated from the ratio of the aromatic and unsaturated (nonaromatic) subunits in the compound.

Stilbene (**16**) and stilbene oligomers (**17**) include fewer double bonds than aromatic subunits. Therefore it is expected that for these compounds the conclusions derived from the aromatic systems will apply more or less. In Figure 7 a comparison of the calculated and experimental spectra for the $1A_g \rightarrow 1B_u$ transitions of **16** and **17** is presented. For **16** the B-P86 functional shows a clear underestimation of the displacement and the spectra obtained with B3-LYP and BH-LYP indicate that about 30−40% of EEX would yield the best agreement with experiment. Good results for ΔE^{0-0} are only obtained with the BH-LYP functional (error of −0.13 eV). A similar conclusion can be drawn from the data calculated for **17** and thus no significant dependence of the optimum amount of EEX on the number of repeating units can be observed in contrast to the findings for the rylenes (see Section 3.2.1).

The simulations for the $1A_1 \rightarrow 1B_1$ transition of diphenylcyclopropenone (**18**), which can be regarded as a derivative of *cis*-stilbene, show an underestimation of the displacement with B3-LYP (see the Supporting Information). The spectrum calculated with the BH-LYP functional is in good agreement with experiment although an even larger amount of EEX seems to be necessary for a quantitative reproduction of the experimental spectrum. With the B-P86 functional, on the other hand, worse results are obtained which show little similarity with the experimental spectrum. Thus, compared to **16** a larger amount of EEX seems to be necessary. This can be explained with the significant participation of the CO group in the electronic excitation process that involves some charge transfer. ΔE^{0-0} seems to increase systematically with increasing EEX included in the functional and BH-LYP gives the best agreement with experiment (error of 0.12 eV).

The results obtained for the $1A_g \rightarrow 1B_u$ transition of azobenzene (**19**) are similar to those obtained for **16**. The B-B86 results are far off; the B3-LYP functional yields a slight underestimation of the displacement while BH-LYP overestimates it indicating that about 30% of EEX would be optimum (see the Supporting Information). These results (and the good performance of BH-LYP for predicting ΔE^{0-0} with a very small error of 0.01 eV) indicate that the behavior of an azo compound (concerning the $\pi \rightarrow \pi^*$ transition) is similar to that of the corresponding hydrocarbon.

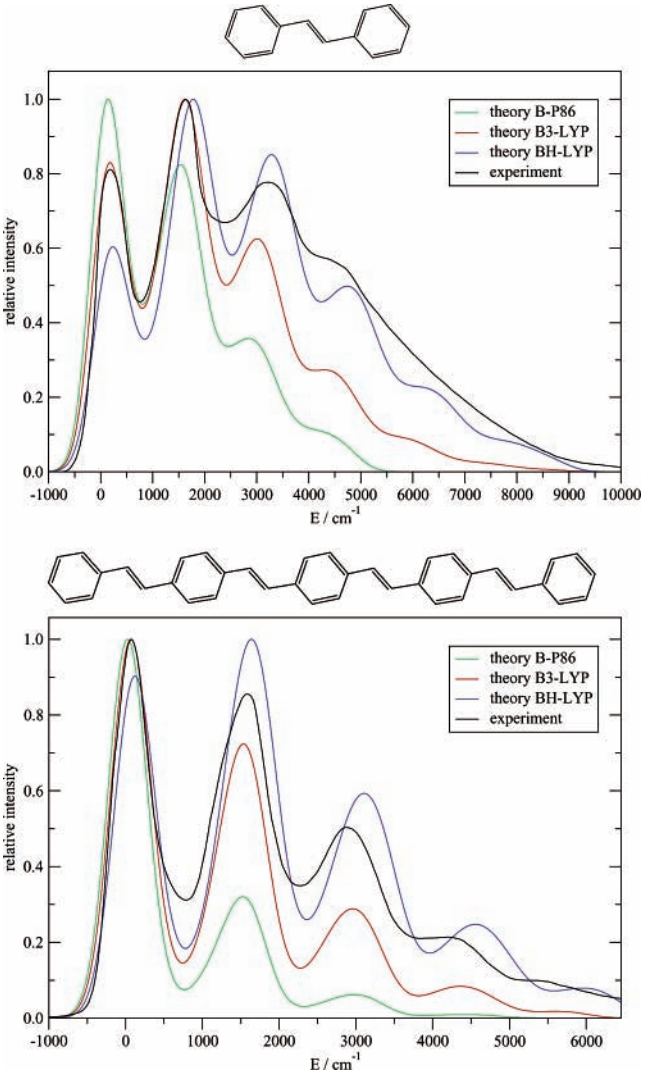

Figure 7. Top panel: Comparison of the calculated and experimental[54] absorption spectra for the $1^1A_g \rightarrow 1^1B_u$ transition of stilbene (**16**). Bottom panel: Comparison of the calculated and experimental[55] absorption spectra for the $1^1A_g \rightarrow 1^1B_u$ transition of **17**.

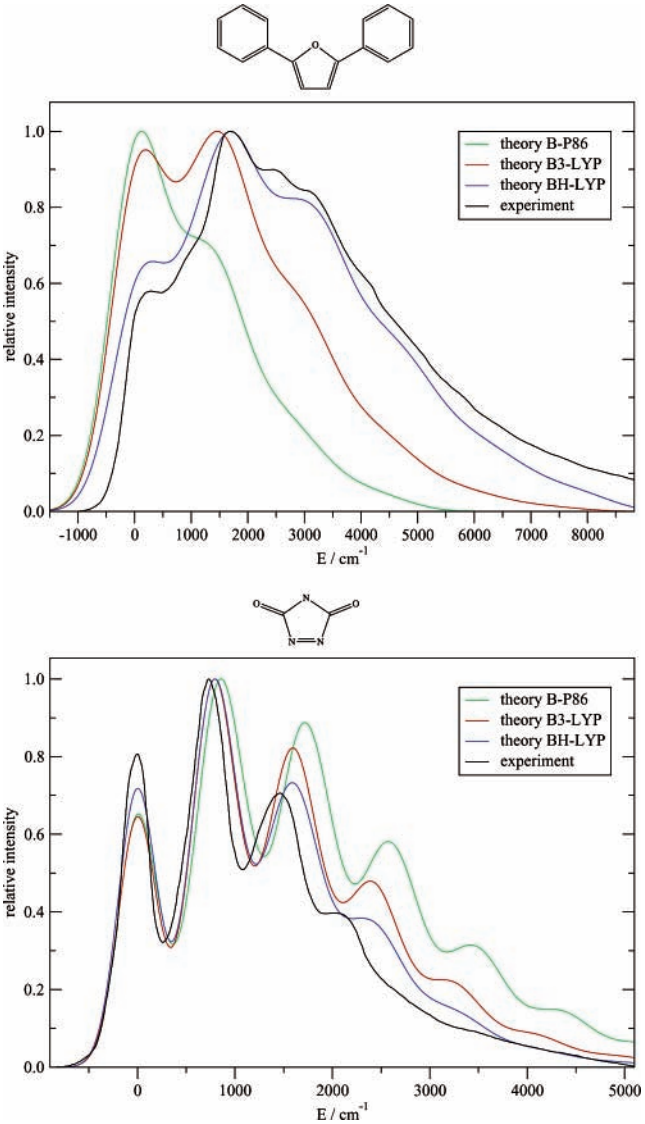

Figure 8. Top panel: Comparison of the calculated and experimental[41] absorption spectra for the $1^1A_1 \rightarrow 1^1B_1$ transition of diphenylfurane (**28**). Bottom panel: Comparison of the calculated and experimental[56] absorption spectra for the $1^1A_1 \rightarrow 1^1B_2$ transition of **30**.

For the $1A_g \rightarrow 1B_{3u}$ state of diphenylacetylene (**20**) both B-P86 and B3-LYP clearly underestimate the displacement (see the Supporting Information). The BH-LYP results are in acceptable agreement with experiment. However, the displacement still seems to be too small and therefore the necessary amount of EEX seems to be larger for **20** when compared to **16**, which is in line with the conclusions discussed for the double and triply bonded systems (see Section 3.2.3). Again, the BH-LYP functional yields the best agreement with experiment regarding the ΔE^{0-0} value, which is in error by only 0.2 eV. A slightly larger EEX value, however, would be better, which correlates with the findings for the simulated spectra.

Diphenylfurane (**28**) consists of three connected aromatic rings and from a formal point of view does not include any double or triple bonds. Therefore, similar results as for the aromatic compounds presented in Section 3.2.1 are expected. In Figure 8 a comparison of the calculated and experimental absorption spectra for the $1A_1 \rightarrow 1B_1$ transition is shown. In contrast to our expectation, both B-P86 and B3-LYP strongly underestimate the displacement while the spectrum calculated with the BH-LYP functional is in very good agreement with experiment. An inspection of the orbitals which are participating in this transition, i.e., the HOMO and LUMO of **28**, reveals an explanation for this puzzling behavior. Due to a nodal plane perpendicular to the molecular plane, the orbital density of the HOMO is zero at the oxygen atom. Furthermore, the LUMO also has very low probability in this region of the molecule and thus the HOMO $\rightarrow$ LUMO excitation of **28** is actually quite similar to that of polyenes. Consequently, a large amount of EEX is necessary for an accurate description of the displacement upon excitation as shown above for the other systems including conjugated double bonds. The ΔE^{0-0} value is predicted very accurately with the BH-LYP functional (error of -0.10 eV), which is in line with the findings for the simulated spectra.

The calculations performed for the $1A_1 \rightarrow 1B_1$ excitation of pentathiophene (**29**) show a significant underestimation of the displacement with B-P86 (see the Supporting Information). The results obtained with B3-LYP and BH-LYP indicate that 30−40% EEX would probably yield the best agreement with the experimental spectrum. This underlines that the conclusions for the rigid aromatic compounds discussed above (see Sections 3.2.1 and 3.2.2) can also be transferred to more flexible molecules built from aromatic subunits. It should be noted that the orbital density of the HOMO is zero at the central sulfur atom due a nodal plane as for the HOMO of **28**. Because the

orbital coefficients of the LUMO are larger and **29** also contains a larger number of aromatic rings this "hidden polyene" effect is less pronounced when compared to **28**. Regarding the errors for ΔE^{0-0} BH-LYP clearly shows the best agreement with the experiment (error of −0.14 eV).

3.2.5. Weakly Dipole-Allowed n → π Transitions.* All the examples presented so far correspond to $\pi \rightarrow \pi^*$ transitions which are of particular importance in many areas of application due to the inherently large transition probabilities. The oscillator strengths for $n \rightarrow \pi^*$ transitions on the other hand are much smaller and thus vibronic coupling (that has been neglected so far) is expected to have a large effect on the calculated vibronic structure. However, in the case of a $n \rightarrow \pi^*$ transition that is energetically well separated from other excited states the coupling is small and the vibronic structure can be described accurately enough within the FC approximation.

As an example we finally we want to discuss the weakly dipole-allowed $n \rightarrow \pi^*$ ($1A_1 \rightarrow 1B_2$) transition of **30**. The TDDFT calculations with the three functionals yield a vertical energy gap to the next higher lying dipole-allowed excited state of 2.4−2.8 eV suggesting that vibronic coupling can safely be neglected. A comparison of the calculated and experimental absorption spectra of **30** is given in Figure 8. In contrast to the $\pi \rightarrow \pi^*$ transitions discussed thus far (with the exception of **10**) the calculations for **30** show a systematic decrease of the displacement with increasing amount of EEX. Furthermore, compared to the $\pi \rightarrow \pi^*$ transitions the dependence of the displacement on EEX seems to be smaller. Both B-P86 and B3-LYP show a slight overestimation of the displacement while the BH-LYP functional is in almost perfect agreement with the experimental spectrum. These results indicate that the conclusions obtained for the $\pi \rightarrow \pi^*$ transitions probably cannot be simply transferred to other types of excited states. The absolute (signed) errors of the ΔE^{0-0} values systematically decrease (increase) with increasing fraction of EEX included in the functional (as for the $\pi \rightarrow \pi^*$ transitions) and BH-LYP gives an excellent agreement with the experiment (error of −0.07 eV), which is in line with the calculated spectra.

3.3. Doublet−Doublet Transitions. Radical species play an important role in numerous fields of scientific research, for example, in the chemistry of biological systems, for environmental (atmospherical) studies, and also in astrophysics. For a large number of technically relevant processes radicals are key intermediates and they have been the subject of intense spectroscopic studies for many years. In the following the results obtained for the doublet−doublet transitions of neutral radicals, radical cations, and radical anions will be presented.

3.3.1. Neutral Radicals. A comparison of the calculated and experimental absorption spectra for the weakly dipole-allowed $1B_2 \rightarrow 1A_2$ transition of the phenoxyl radical (**31**) is shown in Figure 9. In contrast to the $\pi \rightarrow \pi^*$ transitions of the neutral closed-shell compounds (with the exception of **10**) a decrease of the displacement with increasing EEX included can be observed. Furthermore, the influence of EEX on the displacement seems to be smaller when compared to the transitions of the closed-shell systems. Both B-P86 and B3-LYP yield a slight underestimation the displacement while the BH-LYP functional is in good agreement with experiment (except for the small frequency shift). It should be noted that although this transition is only weakly dipole allowed the error due to the neglect of vibronic coupling is small as shown in our previous work.[16] A large influence of EEX on the ΔE^{0-0} value is found (Figure 3 and Table 1) and ΔE^{0-0} systematically increases with the amount of EEX included in the functional. Unlike the findings

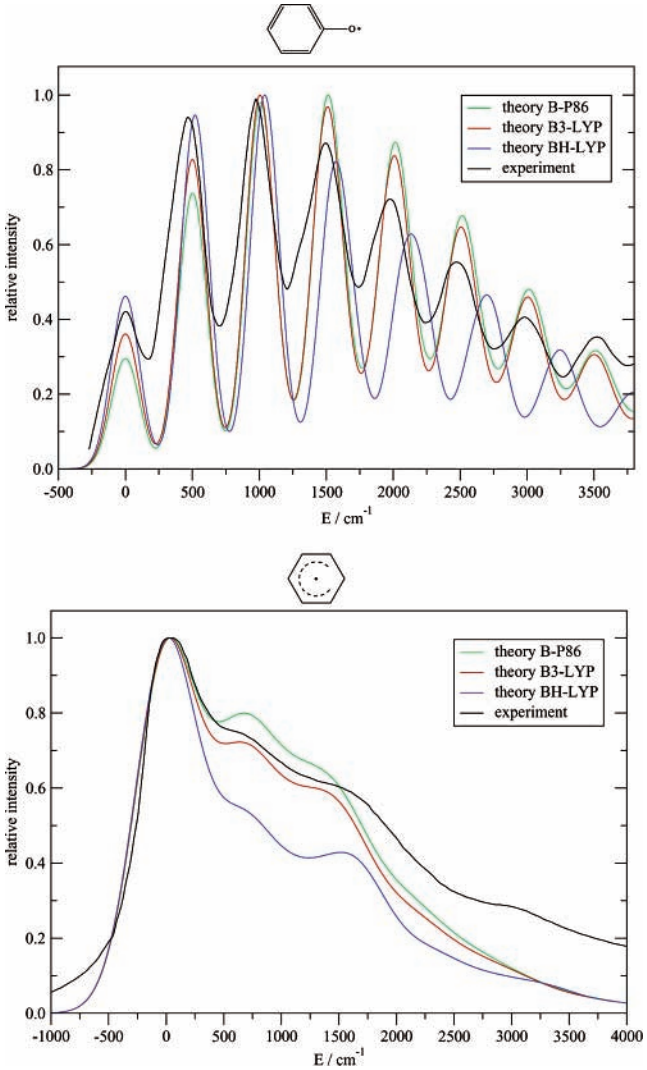

Figure 9. Top panel: Comparison of the calculated and experimental[57] absorption spectra for the $1^2B_2 \rightarrow 1^2A_2$ transition of the phenoxyl radical (**31**). Bottom panel: Comparison of the calculated and experimental[58] absorption spectra for the $1^2B_2 \rightarrow 2^2A_2$ transition of the cyclohexadienyl radical (**32**).

for the simulated spectra the B3-LYP functional gives the best agreement with experiment (error of 0.02 eV).

For the strongly dipole-allowed $1B_2 \rightarrow 2A_2$ transition of the cyclohexadienyl radical (**32**) a comparison of the calculated and experimental absorption spectra is presented in the bottom panel of Figure 9. As for **31** a systematic decrease of the displacement with increasing amount of EEX is seen. The BH-LYP functional clearly underestimates the displacement and an amount of 10−20% EEX is expected to be optimum. In contrast, the errors for ΔE^{0-0} indicate that a portion of 30−40% EEX would yield the best agreement with experiment.

Simulations performed for the strongly dipole-allowed $1B_2 \rightarrow 2A_2$ transition of the benzyl radical (**33**) show similar results as for the iso-electronic phenoxyl radical (see the Supporting Information). The influence of EEX on the displacement upon excitation is rather small but more pronounced for the ΔE^{0-0} value.

3.3.2. Radical Cations. A comparison of the calculated and experimental absorption spectra for the strongly dipole-allowed $1A_u \rightarrow 1B_{3g}$ transition of the naphthalene radical cation (**34**) is shown in Figure 10. The simulations show a strong dependence on the amount of EEX included in the functional and an increase of the displacement with EEX can be observed as for the $\pi \rightarrow$

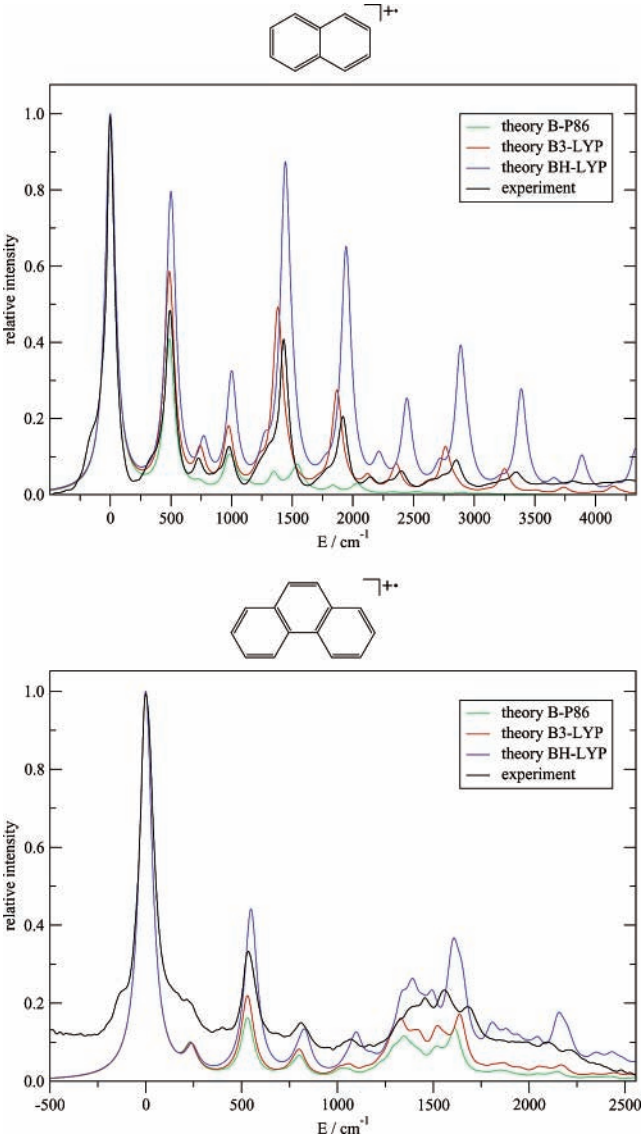

Figure 10. Top panel: Comparison of the calculated and experimental[59] absorption spectra for the $1^2A_u \rightarrow 1^2B_{3g}$ transition of the naphthalene radical cation (**34**). Bottom panel: Comparison of the calculated and experimental[60] absorption spectra for the $1^2B_2 \rightarrow 1^2A_2$ transition of the phenanthrene radical cation (**36**).

π^* transitions of the neutral closed-shell compounds. The B-P86 functional significantly underestimates the displacement while with BH-LYP it is clearly too large. The spectrum obtained with the B3-LYP functional is in almost perfect agreement with experiment. On the contrary, nearly identical results are obtained for the ΔE^{0-0} values with all three functionals (absolute errors of about 0.05 eV, see Figure 3 and Table 1) as opposed to the closed-shell systems. Similar results are also obtained for the radical cations **35**, **36**, and **37** suggesting that the findings presented above are general characteristics of the first strongly dipole-allowed transitions of radical cations of PAH.

For the strongly dipole-allowed $1B_{3g} \rightarrow 1A_u$ transition of the anthracene cation radical (**35**) again the B-P86 functional yields an underestimation and BH-LYP an overestimation of the displacement while the simulation with B3-LYP is in good agreement with experiment (see the Supporting Information). A comparison of the calculated and experimental absorption spectra for the strongly dipole-allowed $1B_2 \rightarrow 1A_2$ transition of the phenanthrene radical cation (**36**) is shown in Figure 10. Compared with the last two examples the influence of EEX on

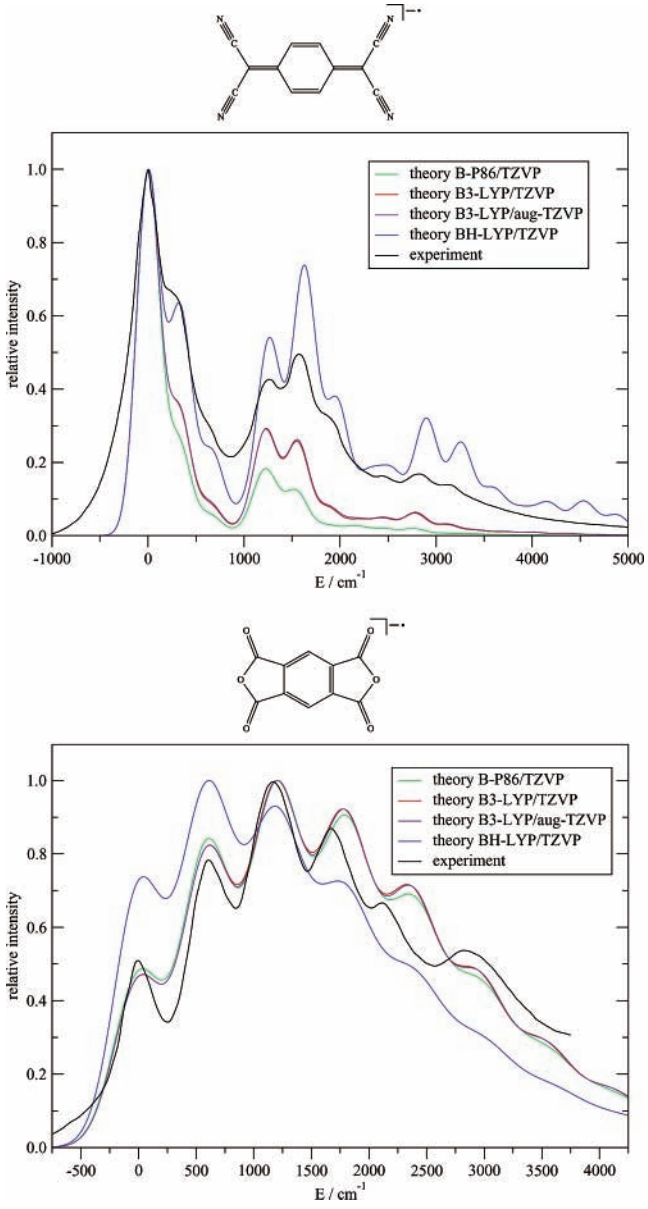

Figure 11. Top panel: Comparison of the calculated and experimental[63] absorption spectra for the $1^2B_{2g} \rightarrow 1^2B_{1u}$ transition of the radical anion **38**. Bottom panel: Comparison of the calculated and experimental[64] absorption spectra for the $1^2A_u \rightarrow 1^2B_{2g}$ transition of the radical anion **39**.

the displacement seems to be even smaller. As before, the spectrum obtained with the B3-LYP functional is in best agreement with experiment.[61]

This also holds for the strongly dipole-allowed $1A_2 \rightarrow 1B_2$ transition of the fluorene radical cation (**37**) (see the Supporting Information). It should be noted that for the two peaks at about 250 and 400 cm^{-1}, respectively, the simulations with all three functionals yield different relative intensities in contrast to the absorption spectrum measured in a neon matrix, which shows a similar intensity for the two peaks. However, the spectrum of **37** obtained under gas-phase conditions[62] shows a larger relative intensity for the peak at 400 cm^{-1} in agreement with our calculations which suggests that these differences can be traced back to perturbation effects of the host matrix.

3.3.3. Radical Anions. In Figure 11 a comparison of the calculated and experimental absorption spectra for the strongly dipole-allowed $1B_{2g} \rightarrow 1B_{1u}$ transition of the radical anion **38** is presented. The simulations clearly show an increase of the

displacement upon excitation with the fraction of EEX included in the functional. Both B-P86 and B3-LYP underestimate the displacement while BH-LYP yields an overestimation. Compared to a simulation based on an UDFT treatment for the ground and excited states at the B3-LYP/aug-cc-pVDZ level[65] the displacement upon excitation seems to be smaller with TDDFT. Compared to the closed-shell systems the errors for ΔE^{0-0} are rather independent of the amount of EEX (which also applies to the radical anions **39**, **40**, and **41**). Both B-P86 and B3-LYP yield an (almost) perfect agreement with experiment (absolute errors smaller than 0.02 eV) while the BH-LYP functional gives a small underestimation of −0.18 eV in contrast to the findings for the simulated spectra.

The electron density of an anion is spatially more extended compared to that of the corresponding neutral system and diffuse basis functions are usually recommended for a proper description of the electronic structure. Therefore, additional calculations have been performed with our standard triple-ζ basis set, which was augmented with a set of diffuse functions taken from Dunnings aug-cc-pVDZ basis sets[66] (aug-TZVP). For the ΔE^{vert} and ΔE^{0-0} values of **38** only small changes (<0.05 eV) are observed and the simulated spectrum is almost identical with that obtained without diffuse basis functions (see Figure 11). Similar results are also seen for the radical anions **39**, **40**, and **41**, which indicates that a basis set of triple-ζ quality already is flexible enough to provide a good description of the excited-state properties of such highly conjugated anions. This is in line with previous findings for the electronic ground state of such systems.[67]

For the calculated spectra of the first strongly dipole-allowed ($1A_u \rightarrow 1B_{3g}$) transition of the radical anion **39** only a rather small dependence on EEX can be observed (see the Supporting Information). As before the simulations show an increase of the displacement with increasing amount of EEX. The B-P86 functional underestimates the displacement and the calculated spectra obtained with B3-LYP and BH-LYP suggest that a portion of 30−40% EEX would be optimum. For ΔE^{0-0} a systematic increase with increasing EEX is observed (Figure 3 and Table 1) and the B3-LYP functional gives a good agreement with the experiment (error of −0.04 eV). The bottom panel of Figure 11 shows a comparison of the calculated and experimental absorption spectra for the second strongly dipole-allowed ($1A_u \rightarrow 1B_{2g}$) transition of **39**. In contrast to the previous two examples no systematic influence of the EEX can be seen. The B-P86 and B3-LYP functionals give almost identical results that are in very good agreement with experiment while BH-LYP clearly underestimates the displacement. Compared to a simulation based on an UDFT-B3-LYP/6-31G* treatment for the ground and excited states,[68] TDDFT seems to yield very similar results. Small errors for ΔE^{0-0} of about 0.25 eV are obtained with all three functionals. The results obtained for two different transitions of **39** show that the optimum amount of EEX depends on the excited state investigated and thus conclusions drawn for a particular transition probably cannot simply be transferred to other excited states.

For the first strongly dipole-allowed ($1A_2 \rightarrow 1B_2$) transition of the radical anion **40** the B3-LYP functional yields the best agreement with experiment (see the Supporting Information). The B-P86 calculation provides results that are only slightly inferior. For the ΔE^{0-0} values only a rather small influence is found and all three functionals yield results that are in very good agreement with experiment (absolute errors smaller than 0.1 eV, see Figure 3 and Table 1). For the second strongly dipole-allowed ($1A_2 \rightarrow 3A_2$) transition of **40** the B-P86 functional seems to give the best agreement with experiment while the displacement seems to be slightly overestimated already with B3-LYP (see the Supporting Information). The dependence of the ΔE^{0-0} values on EEX is larger compared to the first transition. Both B3-LYP and BH-LYP yield a very good agreement with experiment (errors of −0.04 and 0.07 eV, respectively) while the B-P86 result is slightly too low by −0.23 eV.

For the strongly dipole-allowed $1B_2 \rightarrow 1A_2$ transition of the radical anion **41** the B3-LYP functional shows the best agreement with experiment (see the Supporting Information) and also the error for ΔE^{0-0} of −0.01 eV is very small. As for the other radical anions increasing admixture of EEX as in BH-LYP deteriorates the agreement with experiment.

4. Conclusions and Summary

In this paper, we have presented an investigation of the functional dependence of excited-state geometries and normal modes calculated with TDDFT for large molecules. The conclusions are based on a detailed comparison of the vibronic structure of theoretical and experimental absorption spectra because experimental data for excited-state geometries are in general not available.

Calculations performed with different functionals have shown that the vibronic structure critically depends on the fraction of "exact-exchange" (EEX) included in a hybrid functional. This can be traced back to a large influence of the EEX on the geometrical displacement upon excitation. On the contrary, the dependence of the displacement on the local parts of the approximate xc-functionals chosen has been shown to be rather small.

For over 40 different electronic transitions simulations of the vibronic structure have been performed with different amounts of EEX and conclusions have been drawn concerning the optimum fraction of EEX for a proper description of the excited-state geometry. Furthermore, we have discussed a possible correlation of the quality of the simulated spectra with the errors for ΔE^{0-0} obtained with the different functionals. In general, the calculated properties seem to be a smooth function of the admixture of EEX in the series of the functionals B-P86 (0% EEX), B3-LYP (20% EEX), and BH-LYP (50% EEX).

For the singlet−singlet $\pi \rightarrow \pi^*$ transitions presented in Section 3.2, an increase of the displacement upon excitation with increasing amount of EEX included in the functional has been observed. The only exception is the nonalternant PAH azulene (**10**). In contrast, the simulations for the $n \rightarrow \pi^*$ excitation of **30** clearly show a decrease of the displacement with increasing admixture of EEX indicating that the optimum amount of EEX for a proper description of the excited-state geometry depends critically on the character of the electronic transition. Thus, the conclusions obtained for the $\pi \rightarrow \pi^*$ transitions probably cannot be transferred to other types of excited states.

The simulations performed for the L_a transitions of the rigid PAH (see Section 3.2.1) indicate that for **1**−**5**, **8**, and **9** about 30−40% of EEX should be included in the functional. For **6**, about 20% of EEX gives the best results while for **7** a larger fraction of about 50% seems to be necessary. This suggests that for the rylenes the optimum amount of EEX increases with the number of naphthalene units. For the rigid aromatic systems including heteroatoms (see Section 3.2.2) similar results as for the pure PAH are obtained indicating that charge-transfer effects on the quality of the theoretical description are rather small. The simulations for **13**−**14** show that an amount of 30−40%

EEX gives a proper description of the displacement while for **11** a smaller portion of about 20% EEX yields the best results.

In contrast to the aromatic systems, for the compounds **21**−**23** which consist exclusively of alternating double and/or triple bonds (see Section 3.2.3) a larger amount of about 50−60% of EEX is clearly needed. For triply bonded molecules the influence of EEX on the displacement seems to be larger than that for those with double bonds and also a larger amount of EEX seems to be necessary.

For systems that contain both aromatic parts and alternating double or triple bonds (see Section 3.2.4) it has been shown that the optimum amount of EEX can be estimated from the ratio of the number of aromatic and nonaromatic subunits. The simulations for the compounds **24**−**27** which include a large number of double bonds clearly show that a larger fraction of about 50% EEX is needed. Surprisingly, for **28**, which is built exclusively from aromatic rings, also a large amount of EEX of about 50% is necessary, which has been explained by the similarity of the investigated HOMO → LUMO excitation to that of a diene. For molecules which contain only a relatively small number of double or triple bonds an amount of 30−40% EEX gives the best results as shown for **16**, **17**, **19**, and **29**. The simulations performed for **20** show that a larger amount of about 50−60% EEX is necessary, which in comparison to **16** underlines that a larger fraction of EEX is required for triply bonded molecules than for those with double bonds. Furthermore, also for **18** an amount of 50−60% EEX seems to be an optimum, which has been explained by a significant involvement of the CO group in the excitation.

For the investigated singlet−singlet transitions, the errors for the ΔE^{0-0} values in general strongly depend on the fraction of EEX included (Figure 3 and Table 1). The differences between the values obtained with the BH-LYP (50% EEX) and B-P86 (0% EEX) functionals are always positive and reach up to 1.2 eV for **23**. For the investigated $\pi \rightarrow \pi^*$ transitions (with the exception of **10**−**12**) about 40−60% of EEX is necessary to obtain reliable excitation energies. A correlation of the error for ΔE^{0-0} with the quality of the simulated spectrum could be observed only for less than one-third of the singlet−singlet transitions studied (**7**, **9**, **10**, **15**, **20**, **22**, **27**, **28**, and **30**). Thus no reliable conclusions concerning the optimum amount of EEX for an accurate description of the excited-state geometry can be drawn from the results obtained for ΔE^{0-0}.

The simulations performed for doublet−doublet transitions of the neutral radicals **31**−**33** (see Section 3.3.1) show only a rather small influence of EEX on the displacement upon excitation when compared to the investigated singlet−singlet transitions. A systematic decrease of the displacement with increasing fraction of EEX can be observed for **31** and **32** in contrast to findings for the singlet−singlet $\pi \rightarrow \pi^*$ transitions. The optimum amount of EEX ranges from about 50% for **31** to 10−20% for **32** while for **33** the dependence of the displacement is almost negligible. For the ΔE^{0-0} values a relatively large influence of EEX has been found (Figure 3 and Table 1) reaching up to about 1.1 eV for **33** similar to the singlet−singlet transitions.

For the radical cations **34**−**37** studied (Section 3.3.2) a rather large dependence of the displacement on EEX is found. The simulations show a systematic increase of the displacement with the amount of EEX included in the functional as for the singlet−singlet $\pi \rightarrow \pi^*$ excitations. For all four examples a smaller fraction of about 20% has been shown to be optimum suggesting that this conclusion can also be transferred to the first strongly dipole-allowed transition of other PAH radical cations. Compared to the singlet−singlet $\pi \rightarrow \pi^*$ transitions, for ΔE^{0-0} the influence of EEX is only small (<0.2 eV).

The calculations for the doublet−doublet excitations of the radical anions **38**−**41** (see Section 3.3.3) show a systematic increase of the displacement with EEX (with the exception of the second transition of **39**). The optimum amount of EEX ranges from about 20% for **40** and **41** to 30−40% for **38**. The results for the two transitions of **39** show that the portion of EEX needed depends on the nature of the excited state and the findings for a particular transition thus probably cannot be transferred to other excited states. Concerning the errors for ΔE^{0-0} compared to the singlet−singlet transitions only a small influence of EEX (<0.4 eV) can be observed (Figure 3 and Table 1).

In summary, we have shown that the electronic absorption spectra of a wide range of different molecules can successfully be simulated by a full quantum mechanical treatment that is based on (TD)DFT calculations. The results of this study confirm our previous conclusion, that the calculated vibronic structure of an absorption band is easier to predict than the excitation energies ΔE^{0-0}. Although a few rules of thumb concerning the optimum admixture of EEX have been derived, in general no universal amount of EEX seems to exist that gives a uniformly good description for all systems and states. The results show very clearly that an inclusion of EEX in the functional is necessary for an accurate description of the excited-state geometry. Pure density functionals which are computationally more efficient can only be used to obtain a first overview about a spectrum. If all results are considered together, a hybrid functional with about 30−40% of EEX seems to be a good choice. However, we strongly recommend to check in all TDDFT applications carefully the dependence of the calculated properties on the admixture of EEX, which increases the reliability of the theoretical predictions considerably. Note that the error for the displacement upon excitation also transfers to the gradient of the excited state in the FC region, which is of great importance for dynamical simulations of photochemical reactions. In such applications, vibronic structure calculations for the corresponding electronic transition would give clear hints about the applicability of the chosen density functional.

Concerning future work, it would be clearly interesting to investigate the performance of the recently introduced meta-GGA functionals which show very promising results for ground-state properties.[69] New functionals that partition the exchange energy into short- and long-range parts[70] may also represent an interesting alternative for the calculation of excited-state geometries and the simulation of vibronic spectra.

Acknowledgment. We thank Dr. Christian Mück-Lichtenfeld for technical support and F. Furche for providing us a preliminary version of his excited-state TDDFT gradient using the RI approximation. This work has been supported by the International NRW Graduate School of Chemistry and the BASF corporation.

Supporting Information Available: Comparison of the calculated and experimental absorption spectra for the molecules **2**, **4**, **5**, **8**−**15**, **18**−**21**, **24**−**27**, **29**, **33**, **35**, **37**, and **39**−**41**. This material is available free of charge via the Internet at http://pubs.acs.org.

References and Notes

(1) Casida, M. E. Time-dependent density functional response theory for molecules. In *Recent advances in density functional methods*; Chong, D. P., Ed.; World Scientific: Singapore, 1995; Vol. 1.

(2) Gross, E. K. U.; Dobson, J. F.; Petersilka, M. Density functional theory. *Top. Curr. Chem.* **1996**, *181*, 81.
(3) Bauernschmitt, R.; Ahlrichs, R. *Chem. Phys. Lett.* **1996**, *256*, 454.
(4) Casida, M. E.; Jamorski, C.; Casida, K. C.; Salahub, D. R. *J. Chem. Phys.* **1998**, *108*, 4439.
(5) Tozer, D. J.; Handy, N. C. *J. Chem. Phys.* **1998**, *109*, 10180.
(6) Sobolewski, A. L.; Domcke, W. *Chem. Phys.* **2003**, *294*, 73.
(7) Dreuw, A.; Fleming, G. R.; Head-Gordon, M. *Phys. Chem. Chem. Phys.* **2003**, *5*, 3247.
(8) Dreuw, A.; Weisman, J. L.; Head-Gordon, M. *J. Chem. Phys.* **2003**, *119*, 2943.
(9) Dreuw, A.; Head-Gordon, M. *J. Am. Chem. Soc.* **2004**, *126*, 4007.
(10) Grimme, S.; Parac, M. *Chem. Phys. Chem.* **2003**, *4*, 292.
(11) Parac, M.; Grimme, S. *Chem. Phys.* **2003**, *292*, 11.
(12) Cai, Z.-L.; Sendt, K.; Reimers, J. R. *J. Chem. Phys.* **2002**, *117*, 5543.
(13) Van Caillie, C.; Amos, R. D. *Chem. Phys. Lett.* **1999**, *308*, 249.
(14) Van Caillie, C.; Amos, R. D. *Chem. Phys. Lett.* **2000**, *317*, 159.
(15) Furche, F.; Ahlrichs, R. *J. Chem. Phys.* **2002**, *117*, 7433.
(16) Dierksen, M.; Grimme, S. *J. Chem. Phys.* **2004**, *120*, 3544.
(17) Due to a programming error in one of our programs, the progression of the nontotally symmetric normal mode calculated with B3-LYP in ref 16 was overestimated. The corrected spectrum is included in this publication.
(18) Stratmann, R. E.; Scuseria, G. E.; Frisch, M. J. *J. Chem. Phys.* **1998**, *109*, 8218.
(19) Ahlrichs, R.; Bär, M.; Baron, H.-P.; Bauernschmitt, R.; Böcker, S.; Ehrig, M.; Eichkorn, K.; Elliott, S.; Furche, F.; Haase, F.; Häser, M.; Horn, H.; Huber, C.; Huniar, U.; Kattannek, M.; Kölmel, C.; Kollwitz, M.; May, K.; Ochsenfeld, C.; Öhm, H.; Schäfer, A.; Schneider, U.; Treutler, O.; von Arnim, M.; Weigend, F.; Weis, P.; Weiss, H. *TURBOMOLE*, version 5.6; Universität Karlsruhe: Karlsruhe, 2003.
(20) Becke, A. D. *Phys. Rev. A* **1988**, *38*, 3098.
(21) Perdew, J. P. *Phys. Rev. B* **1986**, *33*, 8822.
(22) Becke, A. D. *J. Chem. Phys.* **1993**, *98*, 5648.
(23) Lee, C.; Yang, W.; Parr, R. G. *Phys. Rev. B* **1988**, *37*, 785.
(24) Becke, A. D. *J. Chem. Phys.* **1993**, *98*, 1372.
(25) Slater, J. C. *Phys. Rev.* **1951**, *81*, 385.
(26) Vosko, S. H.; Wilk, L.; Nusair, M. *Can. J. Phys.* **1980**, *58*, 1200.
(27) Perdew, J. P.; Burke, K.; Ernzerhof, M. *Phys. Rev. Lett.* **1996**, *77*, 3865.
(28) Perdew, J. P.; Burke, K.; Ernzerhof, M. *Phys. Rev. Lett.* **1997**, *78*, 1396.
(29) Perdew, J. P.; Ernzerhof, M.; Burke, K. *J. Chem. Phys.* **1996**, *105*, 9982.
(30) Eichkorn, K.; Treutler, O.; Öhm, H.; Häser, M.; Ahlrichs, R. *Chem. Phys. Lett.* **1995**, *242*, 652.
(31) Eichkorn, K.; Weigend, F.; Treutler, O.; Ahlrichs, R. *Theor. Chem. Acc.* **1997**, *97*, 119.
(32) Bauernschmitt, R.; Häser, M.; Treutler, O.; Ahlrichs, R. *Chem. Phys. Lett.* **1997**, *264*, 573.
(33) Schäfer, A.; Huber, C.; Ahlrichs, R. *J. Chem. Phys.* **1994**, *100*, 5829.
(34) The excited-state TDDFT gradient, using the RI approximation, has been kindly provided by F. Furche (unpublished, appearing in TURBOMOLE 5.7).
(35) Neugebauer, J.; Reiher, M.; Kind, C.; Hess, B. A. *J. Comput. Chem.* **2002**, *23*, 895.
(36) Kind, C.; Reiher, M.; Neugebauer, J.; Hess, B. A. *SNF*, version 2.2.1; Universität Erlangen: Erlangen, 2002.
(37) Scott, A. P.; Radom, L. *J. Phys. Chem.* **1996**, *100*, 16502.
(38) Dierksen, M. *FCfast*, version 0.9; Universität Münster: Münster, 2003.
(39) One can, however, not definitely exclude the possibility that an accurate (nonharmonic) treatment of the double minimum potentials might give an even better agreement with the experimental spectra.
(40) Ferguson, J.; Reeves, L. W.; Schneider, W. G. *Can. J. Chem.* **1957**, *35*, 1117.
(41) Berlman, I. B. *Fluorescence Spectra of Aromatic Molecules*, 2nd ed.; Academic Press: New York, 1971.
(42) Platt, J. R. *J. Chem. Phys.* **1949**, *17*, 484.
(43) Schäfer, A.; Horn, H.; Ahlrichs, R. *J. Chem. Phys.* **1992**, *97*, 2571.
(44) Weigend, F.; Furche, F.; Ahlrichs, R. *J. Chem. Phys.* **2003**, *119*, 12753.
(45) Halasinski, T. M.; Weisman, J. L.; Ruiterkamp, R.; Lee, T. J.; Salama, F.; Head-Gordon, M. *J. Phys. Chem. A* **2003**, *107*, 3660.
(46) Karabunarliev, S.; Gherghel, L.; Koch, K.-H.; Baumgarten, M. *Chem. Phys.* **1994**, *189*, 53.
(47) Grimme, S. *Chem. Phys. Lett.* **1993**, *201*, 67.
(48) Scholz, R.; Kobitski, A. Yu.; Kampen, T. U.; Schreiber, M.; Zahn, D. R. T.; Jungnickel, G.; Elstner, M.; Sternberg, M.; Frauenheim, Th. *Phys. Rev. B* **2000**, *61*, 13659.
(49) Sterzel, M.; Andrzejak, M.; Pawlikowski, M. T.; Gawroński, J. *Chem. Phys.* **2004**, *300*, 93.
(50) Kohler, B. E.; Schilke, D. E. *J. Chem. Phys.* **1987**, *86*, 5214.
(51) Slepkov, A. D.; Hegmann, F. A.; Eisler, S.; Elliot, E.; Tykwinski, R. R. *J. Chem. Phys.* **2004**, *120*, 6807.
(52) The considerable (2- to 4-fold) increase of the line width with increasing energy observed in the experiment[81] is not included in our simulations and has to be taken into account when comparing the spectra.
(53) Shima, S.; Ilagan, R. P.; Gillespie, N.; Sommer, B. J.; Hiller, R. G.; Sharples, F. P.; Frank, H. A.; Birge, R. R. *J. Phys. Chem. A* **2003**, *107*, 8052.
(54) Dyck, R. H.; McClure, D. S. *J. Chem. Phys.* **1962**, *36*, 2326.
(55) Oelkrug, D.; Egelhaaf, H.-J.; Gierschner, J.; Tompert, A. *Synth. Met.* **1996**, *76*, 249.
(56) Pocius, A. V.; Yardley, J. T. *J. Am. Chem. Soc.* **1973**, *95*, 721.
(57) Radziszewski, J. G.; Gil, M.; Gorski, A.; Spanget-Larsen, J.; Waluk, J.; Mróz, B. J. *J. Chem. Phys.* **2001**, *115*, 9733.
(58) Shida, T.; Hanazaki, I. *Bull. Chem. Soc. Jpn.* **1970**, *43*, 646.
(59) Andrews, L.; Kelsall, B. J.; Blankenship, T. A. *J. Phys. Chem.* **1982**, *86*, 2916.
(60) Salama, F.; Joblin, C.; Allamandola, L. J. *J. Chem. Phys.* **1994**, *101*, 10252.
(61) The nonzero baseline observed in the experiment is not included in our simulations and has to be taken into account when comparing the spectra.
(62) Pino, T.; Bréchignac, Ph.; Dartois, E.; Demyk, K.; d'Hendecourt, L. *Chem. Phys. Lett.* **2001**, *339*, 64.
(63) Jeanmaire, D. L.; Van Duyne, R. P. *J. Am. Chem. Soc.* **1976**, *98*, 4029.
(64) Shida, T. *Electronic Absorption Spectra of Radical Ions*; Elsevier: Amsterdam, 1988.
(65) Makowski, M.; Pawlikowski, M. T. *Chem. Phys. Lett.* **2004**, *388*, 367.
(66) Kendall, R. A.; Dunning, T. H., Jr.; Harrison, R. J. *J. Chem. Phys.* **1992**, *96*, 6796.
(67) Treitel, N.; Shenhar, R.; Aprahamian, I.; Sheradsky, T.; Rabinovitz, M. *Phys. Chem. Chem. Phys.* **2004**, *6*, 1113.
(68) Andruniow, T.; Pawlikowski, M.; Zgierski, M. Z. *J. Phys. Chem. A* **2000**, *104*, 845.
(69) Staroverov, V. N.; Scuseria, G. E.; Tao, J.; Perdew, J. P. *J. Chem. Phys.* **2003**, *119*, 12129.
(70) Tawada, Y.; Tsuneda, T.; Yanagisawa, S.; Yanai, T.; Hirao, K. *J. Chem. Phys.* **2004**, *120*, 8425.
(71) Sakamoto, Y.; Suzuki, T.; Kobayashi, M.; Gao, Y.; Fukai, Y.; Inoue, Y.; Sato, F.; Tokito, S. *J. Am. Chem. Soc.* **2004**, *126*, 8138.
(72) Nijegorodov, N.; Mabbs, R.; Downey, W. S. *Spectrochim. Acta, Part A* **2001**, *57*, 2673.
(73) Grimme, J.; Scherf, U. *Macromol. Chem. Phys.* **1996**, *197*, 2297.
(74) Lou, Y.; Chang, J.; Jorgensen, J.; Lemal, D. M. *J. Am. Chem. Soc.* **2002**, *124*, 15302.
(75) Hurst, J. K.; Wormell, P.; Krausz, E.; Lacey, A. R. *Chem. Phys.* **1999**, *246*, 229.
(76) Ohshima, Y.; Fujii, T.; Fujita, T.; Inaba, D.; Baba, M. *J. Phys. Chem. A* **2003**, *107*, 8851.
(77) Mazaki, Y.; Kobayashi, K. *Tetrahedron Lett.* **1989**, *30*, 3315.
(78) Guo, X.; Gan, Z.; Luo, H.; Araki, Y.; Zhang, D.; Zhu, D.; Ito, O. *J. Phys. Chem. A* **2003**, *107*, 9747.
(79) Takeuchi, S.; Tahara, T. *J. Chem. Phys.* **2004**, *120*, 4768.
(80) Luňák, S., Jr.; Nepraš, M.; Hrdina, R.; Mustroph, H. *Chem. Phys.* **1994**, *184*, 255.
(81) Leopold, D. G.; Vaida, V.; Granville, M. F. *J. Chem. Phys.* **1984**, *81*, 4210.
(82) Itoh, T. *J. Chem. Phys.* **2003**, *119*, 4516.
(83) Bartocci, G.; Spalletti, A.; Becker, R. S.; Elisei, F.; Floridi, S.; Mazzucato, U. *J. Am. Chem. Soc.* **1999**, *121*, 1065.
(84) Connors, R. E.; Ucak-Astarlioglu, M. G. *J. Phys. Chem. A* **2003**, *107*, 7684.
(85) Szczepanski, J.; Vala, M.; Talbi, D.; Parisel, O.; Ellinger, Y. *J. Chem. Phys.* **1993**, *98*, 4494.
(86) Shida, T.; Iwata, S.; Imamura, M. *J. Phys. Chem.* **1974**, *78*, 741.
(87) Fabre, P.-L.; Dumestre, F.; Soula, B.; Galibert, A.-M. *Electrochim. Acta* **2000**, *45*, 2697.